Chaotic Regime of Alfvén Eigenmode Wave-Particle Interaction

R. F. Heeter*
Princeton Plasma Physics Lab and JET Joint Undertaking, P.O. Box 451, Princeton, New Jersey 08543

A. F. Fasoli
MIT Plasma Science and Fusion Center, 175 Albany Street, Cambridge, Massachusetts 02139

S. E. Sharapov
JET Joint Undertaking, Abingdon, Oxfordshire OX14 3EA, United Kingdom
(Received 13 March 2000)

The chaotic regime in Alfvén eigenmode wave-particle interaction is identified for the first time in the tokamak plasma of the Joint European Torus. The Alfvén modes are driven by energetic hydrogen minority ions produced by ion cyclotron resonance heating. The experimental signatures of the chaotic regime include spectral broadening, phase flips, and nonperiodic amplitude variations. These phenomena are found to be consistent with a general nonlinear theory of kinetic instabilities near stability threshold developed by Berk, Breizman, and Pekker.

PACS numbers: 52.35.Mw, 52.35.Bj, 52.35.Nx, 52.55.Fa

The physics of Alfvén eigenmodes (AEs) [1] destabilized by resonant fast ions is of interest in both magnetic fusion and nonlinear physics. Unstable AEs may eject energetic fusion α particles from the plasma and impair reactor performance [2–5]. Advances in linear AE physics enable predictions of AE stability limits and diagnosis of the background plasma and fast particles from AE observations [6–8]. AEs also provide a paradigm-testing case for nonlinear wave-particle interaction physics, since fast ions primarily affect an AE's growth rate rather than its structure or frequency [7]. Finally, since AEs are typically resonant with fusion-born α particles, nonlinear AE-particle interactions might be used to diagnose or perhaps even control the αs in burning plasmas [9–11].

Different regimes of nonlinear AE-particle interaction are predicted by a general model formulated by Berk, Breizman, and Pekker (BBP) for kinetic instabilities near stability threshold [12–14]. The model dynamically balances the stabilizing influence of the mode (which flattens the distribution function) against processes which generate the unstable distribution (in the absence of the mode) and tend to restore it (in the presence of the mode). Two key parameters are the net linear drive in the absence of the mode, γ, and the effective collision rate restoring the distribution, ν_{eff}. The regime of AE mode splitting and amplitude modulation was recently identified in data from ion cyclotron resonance heating (ICRH)-driven toroidicity-induced AEs (TAEs) in the Joint European Torus (JET) tokamak [7], and agreement between the data and the model enabled estimates of γ and ν_{eff}.

In this Letter, we report the first experimental identification of the more strongly nonlinear chaotic regime in AE-particle interaction. The nonlinear BBP model is again used to interpret the data and estimate γ and ν_{eff} over a much wider parameter range. The AEs are driven by ICRH of minority hydrogen in majority deuterium plasmas at JET ($n_{\mathrm{H}}/n_{\mathrm{D}} \approx 2\%$), and detected by an 8-channel, 1 MHz, 4 s edge magnetic probe diagnostic [11,15]. To reach strongly nonlinear AE regimes, optimized shear (OS) plasmas are employed [16], as they are less stable to ICRH-driven AEs [11,17].

Figure 1 shows the magnetic fluctuation spectrogram early in a JET OS plasma. During the preheat phase (44–45 s), TAEs are destabilized with only 2 MW of ICRH power. TAEs are common at JET and are identified by their adherence to the TAE dispersion relation [4, 5, 7, 11]. Discrete TAEs ($n = 1$ up to 7) appear in the preheat phase of other JET OS discharges with only 1 MW of ICRH [17], so at 2 MW the TAE drive is relatively strong.

Figure 1 reveals several new TAE phenomena. First, the TAE activity is broadband rather than discrete in

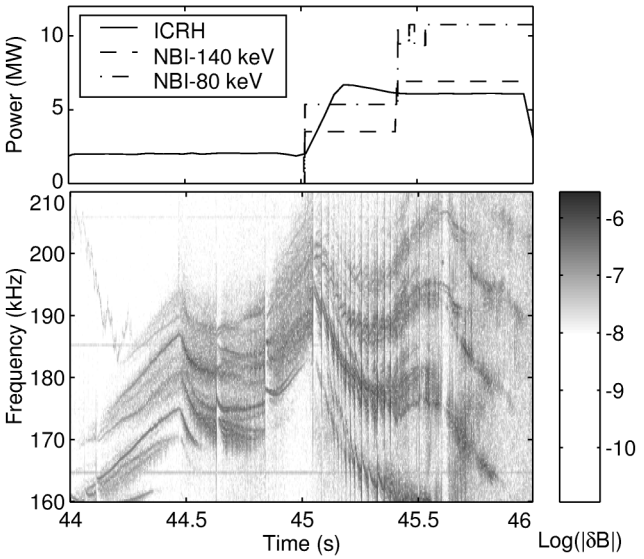

FIG. 1. TAE activity in JET #41629. Top: Auxiliary heating. Bottom: Magnetic fluctuation spectrogram.

frequency; it is difficult to resolve discrete modes as typically seen [7]. Second, our standard method of toroidal mode number analysis, based on fast Fourier transforming (FFTing) data from several toroidal locations and comparing the FFT phases at a given time and frequency, breaks down for these TAEs, even though the signal-to-noise ratio is high and we obtain clear results for TAEs in nearly all other ICRH-heated JET plasmas [11,15]. Third, the line-broadened TAE activity is punctuated by vertical stripes, suggesting rapid events with broad Fourier spectra. These preheat-phase phenomena are seen in 11+ discharges with 2 MW of ICRH, but not with 1 MW. Identical behavior is seen on all available probes, at 4 different toroidal positions. Evidently these are plasma phenomena rather than artifacts of a particular discharge or probe.

Following the BBP model [7], we assume a fast TAE oscillation at a frequency ω_{TAE} and a slowly varying change in the suitably normalized mode amplitude A. We use the mode net growth rate $\gamma = \gamma_{\mathrm{linear}} - \gamma_{\mathrm{damping}}$, and the effective collision rate ν_{eff} mentioned above; the phase angle ϕ (related to the fast-particle contribution to the linear mode frequency) is expected to be small so we set $\phi = 0$ for simplicity. The BBP mode amplitude evolution equation can be written as

$$\frac{dA}{dt} = A - \exp(i\phi)\int_0^{t/2} \tau^2 \int_0^{t-2\tau} \exp[-\nu^3\tau^2(2\tau/3 + \tau_1)]A(t-\tau)A(t-\tau-\tau_1)A^*(t-2\tau-\tau_1)\,d\tau_1\,d\tau\,. \quad (1)$$

Time is normalized to $1/\gamma$, the inverse of the net linear growth rate, and $\nu \equiv \nu_{\mathrm{eff}}/\gamma$. The double integral captures the nonlinear dynamics.

We solved this numerically with MATLAB [18] and benchmarked it against published results from a previous solution for $\phi = 0$ and various ν [11,13,14]. The four main regimes predicted by the BBP model appear in Fig. 2, which replicates Fig. 2 of [13]. Plot A shows steady-state saturation; in this regime agreement was found between the theory and ICRH-driven TAEs in Tokamak Fusion Test Reactor [5,14,19]. When we raise the normalized drive $\gamma/\nu_{\mathrm{eff}} > \gamma_{\mathrm{crit}} = 0.486$ (for $\phi \ll 1$) the theory predicts a transition to periodic limit-cycle behavior (plot B), seen as amplitude modulation in the time domain and sideband formation (pitchfork splitting) in the frequency domain. Further increase in $\gamma/\nu_{\mathrm{eff}}$ leads to a period-doubling transition (not shown). The pitchfork splitting and period-doubling transitions were first observed in JET data, in agreement with the theory [7]. As $\gamma/\nu_{\mathrm{eff}}$ is further increased, BBP theory predicts a period-doubling route to chaotic behavior (plot C), and for the highest $\gamma/\nu_{\mathrm{eff}}$ the model predicts strongly nonlinear, explosive-type behavior (plot D), beyond the scope of this paper [13,14].

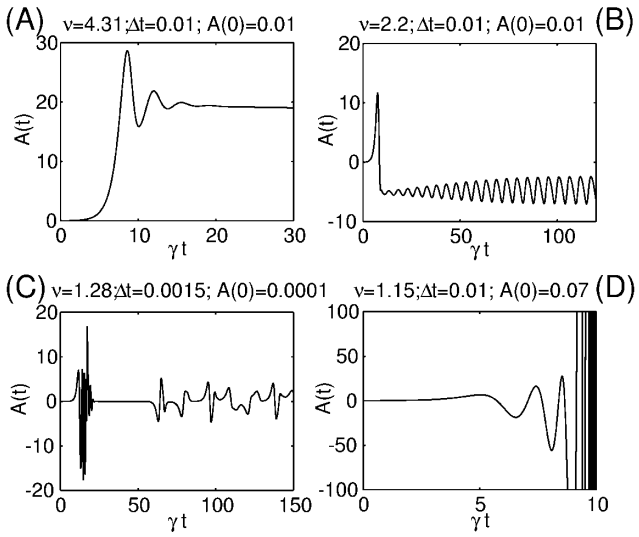

FIG. 2. Normalized mode amplitude (A) vs normalized time γt from Eq. (1) at 4 values of $\nu = \nu_{\mathrm{eff}}/\gamma$.

Table I summarizes key time scales. Simulations typically generate $A(t)$ for 100–200 linear growth times [13,14], or 1–10 ms experimentally, comparable to the typical FFT windows used. To compare theory and experiment we construct simulated signals $S(t) = A(t)\cos(\omega_{\mathrm{TAE}}t)$, using typical JET values $\gamma/\omega_{\mathrm{TAE}} \sim 0.01$ [4,20] to return from normalized time to real time.

The TAE phenomena epitomized in Fig. 1 can now be explained in terms of BBP theory in the chaotic regime. Figure 3 illustrates the line broadening of the mode, comparing 10 ms of experimental data with a BBP simulation. The time domain experimental data (not shown) are dominated by a single mode of amplitude $|\delta B_{\mathrm{pol}}/B|_{\mathrm{edge}} \leq 1 \times 10^{-6}$. The 10 kHz broadening is the Fourier response of chaotic, rapid, nonperiodic mode amplitude $A(t)$ variations on γt time scales. The $A(t)$ variations produce no stable symmetric limit-cycle type sidebands, but quasiperiodic variations produce short-duration asymmetric sidebands in both theory and experiment. Matching the $\Delta f \approx 10$ kHz broadening gives one estimate for the net growth rate $\gamma/\omega_{\mathrm{TAE}}$, about 0.04 in this case.

Figure 4 illustrates the same comparison in the time domain, showing 3 ms of raw data, 3 ms of calibrated data run through a 7th order Butterworth 170–200 kHz digital bandpass filter, and 150 γt growth times of simulated data (3 ms of real time at $\gamma = 5 \times 10^4$/s). Both

TABLE I. Experimental and theoretical time scales for a 160 kHz TAE with $\gamma/\omega_{\mathrm{TAE}} \approx 0.01$.

Variable	Represents	Typical value
$1/f_{\mathrm{sample}}$	Diagnostic sample interval	1×10^{-6} s
$1/f_{\mathrm{TAE}}$	TAE period	6×10^{-6} s
$1/\gamma$	Linear growth time	10^{-4} s
$t_{\max}$	Simulation duration	10^{-3}–10^{-2} s
$n_{\mathrm{FFT}}/f_{\mathrm{sample}}$	FFT window	1–4 $\times 10^{-3}$ s
N/f_{sample}	Spectrogram	0.1–4 s

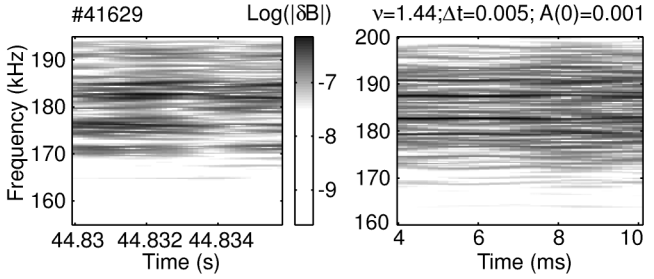

FIG. 3. Spectrograms of chaotic TAEs using 4096-point FFTs. Left: Experiment. Right: Simulation for $\gamma/\omega = 0.043$.

experiment and theory have similar amplitude-variation signatures, and the periodic amplitude oscillations seen in the pitchfork-splitting regime are absent. Any 3 ms segment taken from 30 ms of simulated data (or 1000 ms of experimental data) looks similar, but no segment matches any other, so we do not expect the model to exactly reproduce the experimental data.

From Fig. 4 γ and ν_{eff} may be readily extracted. Simply being in the chaotic regime constrains $1.25 < \nu < 2.0$. Meanwhile, the filtered experimental data show 20–30 peaks in $A(t)$ over 3 ms, or 7–10 peaks/ms. The simulation has 20–30 peaks in 150 growth times $1/\gamma$. At 6 growth times per peak, 7–10 peaks/ms suggest $\gamma = 4\text{–}6 \times 10^4/\text{s}$, 5–7 times larger than found previously for pitchfork splitting in plasmas with standard current profiles [7], but qualitatively consistent with the different density and current profiles in an OS plasma [11]. The observed 185 kHz mode frequency leads to $\gamma/\omega \approx 0.034$ to 0.052 and $\nu_{\text{eff}} = \gamma\nu \sim 5\text{–}12 \times 10^4/\text{s}$, 3–7 times larger than in the pitchfork-splitting case [7], but also qualitatively consistent with expectations for OS plasmas.

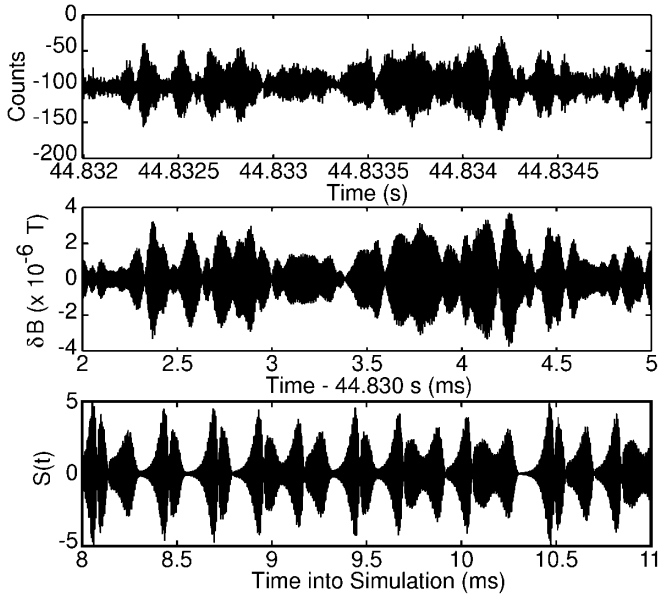

FIG. 4. 3 ms TAE signal comparison. Top: Raw data. Middle: Bandpass-filtered calibrated data. Bottom: Simulated signal for a chaotic AE with $\gamma/\omega_{\text{TAE}} = 0.043$.

We also note another signature for the chaotic and explosive regimes, namely the effect of the repeated inversion of $A(t)$ evident in Fig. 2, which has not been emphasized in the literature. Experimentally, the AE mode amplitude sometimes drops to essentially zero, and at these times the TAE often phase shifts by π, as exemplified in Fig. 5. All phase flips are seen by all probes. From $S(t) = A(t)\cos(\omega_{\text{TAE}}t)$ these phase flips are the predicted amplitude inversions. They occur only when the $A(t)$ tracks through zero, and not when it simply becomes small and recovers, as seen by considering the two functions $S(t) = A(t)\cos(t/10)$ and $S(t) = |A(t)|\cos(t/10)$ with $A(t) = t/50 - 10$.

In addition to the phase flip at 44.832 03 s, at least 10 additional experimental phase flips exist in the interval up to 44.8417 s. The average interval between flips is therefore about 1.08 ms, whereas typical FFT windows used in our data analysis software are 1.024, 2.048, or 4.096 ms, so phase flips are frequent enough to affect most FFTs. The phase flips break the coherence of the mode, so FFTs from windows containing phase flips do not properly measure the phase of the mode, causing our standard mode-number analysis to break as described above. Toroidal mode numbers and peak mode amplitudes can still be determined using bandpass-filtered signals from different probes. Mode numbers thus obtained agree with our standard algorithm in the prechaotic BBP regimes.

Figure 6 illustrates the full nonlinear progression from mode destabilization through chaotic behavior for a different discharge, where ICRH heating was not applied until the main neutral beam heating phase. In contrast with the ICRH-preheated plasmas, no ICRH-driven fast ions are present to destabilize AEs prior to the data acquisition. The ICRH power ramp leads to a progressive increase in the fast ion drive, causing TAEs to grow, pitchfork, period double, and then go chaotic within 300 ms (much shorter than the current diffusion time). Figure 7 plots 20 ms segments of bandpass-filtered $n = 4$ TAE data, starting at (a) 44.230 s (140–150 kHz filter), (b) 44.265 s (135–145 kHz), (c) 44.300 s (133–143 kHz), and (d) 44.500 s (127–137 kHz), showing the (a) steady-state saturation, (b) amplitude modulation, (c) period doubling transition to chaos, and (d) fully chaotic regimes of the AE, respectively. The mode amplitude

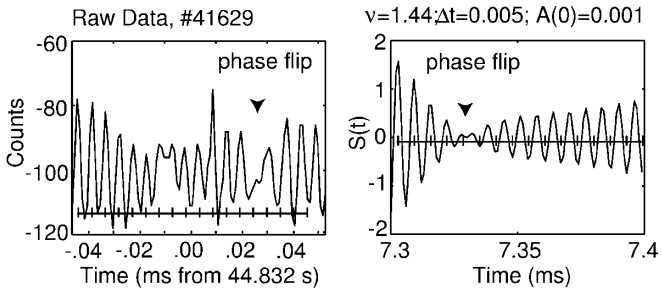

FIG. 5. Phase flips. Left: Experiment. A half-period shift occurs only at $t \approx +0.03$ ms. Right: Simulation.

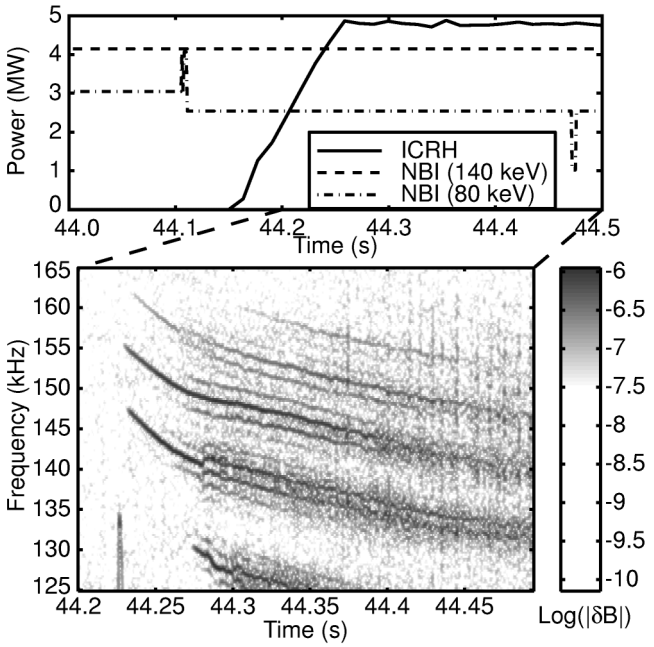

FIG. 6. Auxiliary heating and magnetic fluctuations, JET #49447. The TAEs have toroidal mode numbers $n = 3$ to 6.

variation of less than a factor of 2 is consistent with theory.

In summary, the experimental data presented here identify for the first time a fast-particle-driven plasma instability in the chaotic regime. The observed features agree with predictions of the Berk-Breizman-Pekker model, including rapid, nonperiodic variation in mode amplitudes, and phase flips due to mode-amplitude inversions. Hints of explosive-type behavior beyond the chaotic regime, such as the fast events (vertical stripes) in spectra as in Fig. 1 where the amplitude increases by an order of magnitude, will be analyzed elsewhere [17]. Characterizing the nonlinear state of the AEs yields information about the fast particle population (through the mode growth rate) and the ICRH-induced diffusion (which dominates the effective collision rate ν_{eff}). We note that if future optimized shear experiments use deuterium-tritium plasmas without ICRH, the effective collision rate for fusion alpha particles should be much smaller than it has been for ICRH-accelerated ions. This implies the minimum growth rate, γ, for alpha particle driven modes to reach the chaotic and explosive regimes ($\nu \equiv \nu_{\text{eff}}/\gamma < 2.0$) should be reduced compared to the ICRH-heated plasmas discussed here. Conversely, any strongly nonlinear AEs (which might cause fast ion confinement problems) might be controlled by using other waves resonant with the alphas to drive up ν_{eff} and thus ν.

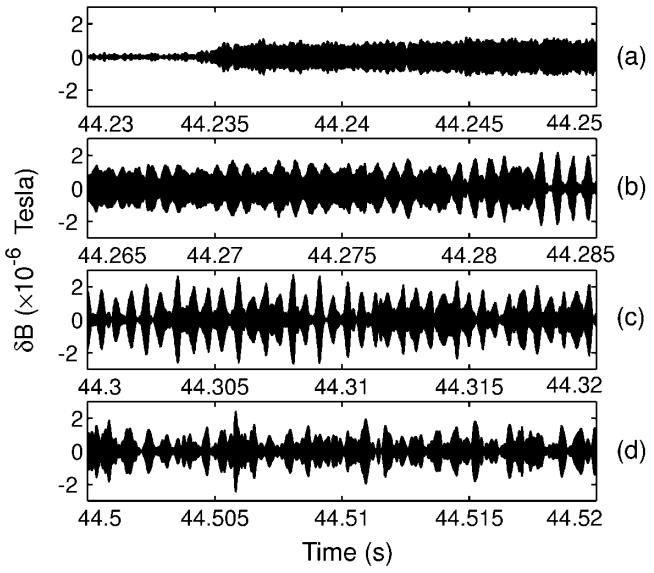

FIG. 7. Calibrated, bandpass-filtered magnetic fluctuations from four phases of JET #49447, shown to scale.

We thank Dr. C. Gormezano, Dr. J. Jacquinot, and JET for experimental support, and Dr. B. Breizman and Dr. H. Berk for useful discussions. This research was supported by EURATOM (JET), the Centre des Recherches en Physique des Plasmas (A. F. from Lausanne, Switzerland), U.S. DOE Contract No. DE-AC02-76-CHO3073 (R. H. from PPPL), U.S. DOE Contract No. DE-FG02-99-ER54563 (A. F. from MIT), the Fanny and John Hertz Foundation (R. H.), and completed under the auspices of the U.S. DOE by UC LLNL (R. H.) under Contract No. W-7405-Eng-48.

*Present address: LLNL, L-043, P.O. Box 808, Livermore, CA 94551.

[1] C. Z. Cheng, L. Chen, and M. S. Chance, Ann. Phys. (N.Y.) **161**, 21 (1985).
[2] K. L. Wong *et al.,* Phys. Rev. Lett. **66**, 1874 (1991).
[3] W. W. Heidbrink *et al.,* Nucl. Fusion **31**, 1635 (1991).
[4] A. Fasoli *et al.,* Plasma Phys. Controlled Fusion **39**, B287 (1997).
[5] K. L. Wong, Plasma Phys. Controlled Fusion **41**, R1 (1999).
[6] L. G. Eriksson *et al.,* Phys. Rev. Lett. **81**, 1231 (1998).
[7] A. Fasoli *et al.,* Phys. Rev. Lett. **81**, 5564 (1998).
[8] A. Fasoli *et al.,* Phys. Plasmas **7**, 1816 (2000).
[9] N. J. Fisch and M. C. Herrmann, Nucl. Fusion **34**, 1541 (1994).
[10] M. C. Herrmann and N. J. Fisch, Phys. Rev. Lett. **79**, 1495 (1997).
[11] R. F. Heeter, Ph.D. thesis, Princeton University, 1999.
[12] H. L. Berk, B. N. Breizman, and M. S. Pekker, Phys. Rev. Lett. **76**, 1256 (1996).
[13] H. L. Berk, B. N. Breizman, and M. S. Pekker, Plasma Phys. Rep. **23**, 778 (1997).
[14] B. Breizman *et al.,* Phys. Plasmas **4**, 1559 (1997).
[15] R. F. Heeter, A. F. Fasoli, S. Ali-Arshad, and J. M. Moret, Rev. Sci. Instrum. (to be published).
[16] C. Gormezano *et al.,* Phys. Rev. Lett. **80**, 5544 (1998).
[17] R. F. Heeter, A. F. Fasoli, and S. E. Sharapov, Phys. Plasmas (to be published).
[18] MATLAB, 5th ed., The MathWorks, 1997.
[19] K. L. Wong *et al.,* Phys. Plasmas **4**, 393 (1997).
[20] W. Kerner *et al.,* Nucl. Fusion **38**, 1315 (1998).